13th Australasian Fluid Mechanics Conference
Monash University, Melbourne, Australia
13-18 December 1998

NUMERICAL PREDICTION OF FLOW OVER A TRIANGULAR, STREAMLINED WEIR

J.E. Sargison and J.S. Montes

Department of Civil and Mechanical Engineering
University of Tasmania, Hobart, Tasmania, AUSTRALIA

ABSTRACT

The flow of water over a streamlined weir was modelled using numerical techniques to solve the fundamental equations of potential flow. The solution was based on a transformation of the physical, (x,y) plane, to the stream function plane (φ,ψ), which produced a regular, rectangular grid for the finite difference solution of Laplace's equation for the depth y in terms of the stream function ψ and the potential function φ. The assumption of constant energy was used as a second condition of the solution and the assumed upstream energy was obtained from an experimental value, which was tested in the final stage of the analysis by the comparison of momentum upstream and at the crest of the weir.

The numerical output of the potential flow solution included the flow surface profile, as well as velocity and pressure profiles at several cross sections. These calculated values were found to compare well with equivalent, experimentally measured profiles at several flow rates.

1 NOMENCLATURE

p = water pressure
q = water discharge rate per unit width
Re = Reynolds number
u = longitudinal velocity, parallel to the x direction
V = streamline velocity (m/s)
V_s = surface streamline velocity (m/s)
v = transverse velocity, parallel to the y direction (m/s)
y_c = critical depth of flow
y_s = height of the water surface above the channel bottom (m)
z = height of weir surface above channel bottom (m)
β = slope angle of weir (20°)
ϕ = hydrodynamic potential (m2/s)
ψ = stream function (m2/s)
ν = kinematic viscosity of the flow (m2/s)
* = dimensionless variable
γ = ρg = specific gravity (N/m3)

2 INTRODUCTION

The solution of the flow over the streamlined weir has a number of points of interest. The selection of a streamline shape for the weir removes the complication of separation at the lower boundary. The focus of the solution was the region of highest curvature of the streamlines at the crest of the weir, which was complicated by the occurance of critical flow in this region. Numerical smoothing techniques were introduced to stabilise the solution of the governing equations of the flow.

The methods of solution developed by THOM and APPELT (1961), LAUCK (1925) and MONTES (1996) were based on a transformation from the x, y plane to the ϕ, ψ plane in a similar manner to the current method.

The use of smoothing and the principal of momentum conservation have been extensions of previous work. The use of a general shape for the lower profile of the weir and the steady convergence to a solution verified by experiment indicate that there is potential for the program to be used for other, similar weir shapes.

3 METHOD OF SOLUTION

3.1 Weir Shape

The weir design (fig. 1) is based on shape data obtained from a streamlined weir example presented by DOMINGUEZ.

The weir used for experimental verification was made according to the mathematical model shape without sudden changes in profile or curvature and incorporating gradual fairings where the channel bottom was intersected.

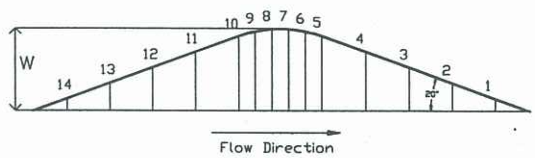

Figure 1: Shape of weir

3.2 Governing Equations

The solution of the model is governed by the equations of potential flow, i.e. inviscid and irrotational flow with constant energy E. The following conditions are used in the flow calculation.

3.2.1 Continuity Equation

$$\frac{du}{dx}+\frac{dy}{dy}=0$$

3.2.2 Laplace's Equation

In the ϕ, ψ plane (ref. Mapping), the dependent and independent variables are interchanged, so that Laplace's equation for y reads:

$$\nabla^2 y = \frac{\partial^2 y}{\partial \phi^2} + \frac{\partial^2 y}{\partial \psi^2}$$

3.2.3 Bernoulli Equation (Conservation of Energy)

$$E = y + \frac{p}{\gamma} + \frac{V^2}{2g}$$

3.2.4 Conservation of Momentum

In the absence of boundary shear, momentum is conserved between all sections of the flow. This condition was used to verify the upstream energy for a given discharge.

3.2.5 Cauchy – Riemann Equations

$$\frac{\partial x}{\partial \phi} = \frac{\partial y}{\partial \psi}$$

3.3 Mapping

A transformation of the x, y plane to the ϕ, ψ plane was used to simplify the solution of the equations of the flow by numerical methods. This method is described in detail by THOM and APELT. By this transformation the flow profile is transformed into a rectangular strip in order to simplify the solution to a rectangular, evenly spaced and simply defined grid.

3.4 Boundary Conditions

3.4.1 Free Surface

The upstream head and total energy of the flow were taken from the experimental results of DOMINGUEZ for a streamlined weir of similar shape, namely: $h = 1.4596\ y_c$

The zero pressure condition at the free surface is used in the calculation of the free surface depth.

The free surface condition is $E = y_s + \frac{V^2{}_s}{2g}$

or in non dimensional form :

$$E^* = \frac{E}{y_c} = \frac{y_s}{y_c} + \frac{V_s^2}{2V_c^2} = y_s^* + \tfrac{1}{2}V_s^*$$

where * denotes non dimensional form. Here E is the total energy and V_s is the surface streamline velocity. The velocity components of V_s are determined from the Jacobian of the inverse mapping:

$$V_s^2 = u^2 + v^2 \; ; \; u = V_s^2 \frac{\partial y}{\partial \psi} \; ; \; v = V_s^2 \frac{\partial y}{\partial \phi}$$

$$\Rightarrow V_s = \frac{1}{\sqrt{\left(\frac{\partial y}{\partial \phi}\right)^2 + \left(\frac{\partial y}{\partial \psi}\right)^2}} \, ,$$

thus the boundary condition is:

$$y_s{}^* = E^* - \tfrac{1}{2}\frac{1}{\sqrt{\left(\frac{\partial y^*}{\partial \phi^*}\right)^2 + \left(\frac{\partial y^*}{\partial \psi^*}\right)^2}}$$

3.4.2 Free Surface Correction Algorithm

The initial surface profile is corrected in steps to attain the correct free surface zero pressure condition outlined above.

The difference between the local energy and the total energy is: $\Delta E = E_{tot} - E_{local}$

The required change in surface depth y_s to make ΔE approach zero, is computed from Taylor's Expansion of $E(y_s)$ about $y = y_s$:

$$E(y_s + \delta H) = E_{tot} = E(y_s) + \frac{dE_{ys}}{dy_s}\delta H + O(\delta H^2)$$

Calculating the derivatives required and substituting we obtain

$$\delta H = \frac{E_{tot} - E(y_s)}{\frac{dEy_s}{dy_s}} = \frac{\Delta E}{1 - \frac{3}{2}\frac{V^2}{g}\frac{u}{\Delta\psi}} \, ,$$

The corrected surface points are:

$$y_{new} = y_{surface} + \delta H$$

An under relaxation coefficient is used in this correction, to stabilise any changes (m=0.5):

$$y'_{surface} = m y_{surface} + (1-m) y_{new}$$

where $y'_{surface}$ is the new surface height.

Near the position of critical depth, repeated application of the smoothing algorithm was required to stabilise the profile.

3.4.3 x Coordinates of surface points

The x coordinates of surface points were calculated by integration of the surface profile slope from the fixed point (x, ϕ) = (0,0) at the end of the weir, upstream along the profile.

It can be shown that

$x - x_0 = \int_{y_0}^{y} \frac{1}{\frac{\partial \psi}{\partial \phi}} dy$, where $x_0 = 0$ and y_0 = water surface height at the end of the weir.

3.4.4 Initial water surface profile

Surface profile curves predicted using energy and backwater methods were joined to form an initial estimate of the water surface profile. The curves were joined near the crest, where y was assumed to be equal to y_c and were smoothed using the cubic smoothing algorithm developed by LEFARA. A polynomial approximation to this profile was used in the program to generate the first set of surface grid points.

3.4.5 Initial x, ϕ relationship along weir profile (bottom)

The initial x, ϕ relationship was estimated from an approximation to the definition of the local velocity, u and the initial free surface profile.

We have: $u = \frac{\partial \phi}{\partial x} \approx \frac{q}{h}$, $\therefore \phi \approx \int_0^x \frac{q}{h} dx$

or, in dimensionless terms, $\phi^* \approx \int_0^{x^*} \frac{1}{h^*} dx^*$

Numerical integration of the equations was used to calculate points (ϕ, x) and the relationship was inverted to a polynomial approximation x = f(ϕ)

3.4.6 Correction of the x, ϕ estimate to fit boundary conditions

Along the boundary, $u = \frac{\partial \phi}{\partial x}$ and $\frac{v}{u} = \frac{dy}{dx}$.

The velocity equations:

$V^2 = u^2 + v^2 = u^2\left(1 + \left(\frac{dy}{dx}\right)^2\right)$ and $u = V^2 \frac{\partial y}{\partial \psi}$ are combined to obtain:

$$\frac{\partial \phi}{\partial x} = u = \frac{1}{\left(1 + \left(\frac{dy}{dx}\right)^2\right)\frac{\partial y}{\partial \psi}}$$

, which can be arranged to the expression:

$$x = \int \left(1 + \left(\frac{dy}{dx}\right)^2\right)\frac{\partial y}{\partial \psi}\partial \phi$$

which determines the location of the fixed boundary points.

An under relaxation coefficient was used to stabilise the correction of x.

3.4.7 End boundaries

The water surface heights and height of internal streamlines were calculated for the upstream and downstream end boundaries from the energy equation. These points were not changed in the iteration process.

At the upstream end of the profile, the flow was uniform and the streamlines horizontal. The internal streamlines were set at equal intervals between the upper and lower boundaries.

As $u = \frac{\partial \psi}{\partial y} = U_0 \Rightarrow y = \frac{\psi}{U_0} = \frac{\psi}{q} h_0$

that is, the height of a streamline is proportional to the value of the stream function ψ.

Two methods were applied to the downstream boundary, namely an assumption of a hydrostatic pressure distribution at the end of the weir, and a vortex to model the curvature of the flow at the end of the weir. By comparison with experiment, it was found that the hydrostatic method was the most accurate.

3.4.8 Downstream boundary approximations

Hydrostatic pressure distribution

The flow was assumed to be uniform at the downstream end of the weir. The fixed position was taken to be at the end of the straight section of the weir. The depth of flow, h at this position was calculated from the energy equation, and the streamlines were located at evenly distributed depths through the flow according to the hydrostatic pressure assumption.

$$E^* = z^* + h^* \cos^2 \beta + \frac{q^2}{2gh^2 \cos^2 \beta}$$

Free Vortex Approximation

The boundary condition at the downstream end of the weir was approximated by a free vortex with radius R to calculate the flow depth and the depth of the streamlines at the downstream boundary.

A free vortex has a velocity distribution described by:

$u = \frac{C}{r} = \frac{C}{R - y}$ from which it can be shown that:

$$\frac{y}{R} = 1 - e^{-\frac{\psi}{q}\frac{q}{c}}$$

The radius chosen for use in the computer program was the value R/y_c = 10, h/R = 0.025 which produced a theoretical pressure closest to the experimental pressure measurement.

3.5 Internal Points

For all internal points, Laplace's equation was satisfied, in the form shown in 3.2.2.

A finite difference formula was applied to the rectangular ϕ,ψ grid formed by the transformation of the x, y plane. Many iterative methods of solution of Laplace's equation in two dimensions for rectangular grid are presented in THOM & APPELT (1961). The '20th Rule' was selected as the appropriate version to use for this application because it is the most accurate of the equations for eight points:

$$y_0 = \frac{1}{20}\left[4(y_1 + y_2 + y_3 + y_4) + (y_5 + y_6 + y_7 + y_8)\right]$$

3.6 Velocity and Pressure profiles

The velocity and pressure profiles, both along the weir and in vertical cross sections of the flow were calculated from the mathematical model and stored in data files. These profiles were compared with the experimental data as verification of the model.

The velocity at any point was calculated from the expression introduced previously in 3.4.1.

The pressure at any point was calculated from the dimensionless form of the Bernoulli equation.

3.7 Momentum Balance

The upstream energy level was selected initially from experimental data on similar weirs and was not corrected in the model solution. The exact energy level can be determined by requiring that the momentum relation be satisfied between any two sections of the mathematical model. The upstream and crest sections were selected as the appropriate sections at which to check the flow momentum.

3.8 Weir surface boundary layer correction

The effect of viscosity on the solution was estimated by using Thwaites' method to estimate the dimensionless displacement thickness of the boundary layer from the calculated velocity distribution along the surface of the weir. The boundary layer was assumed to form only along the bottom weir surface.

The use of a laminar boundary layer correction was justified by the relaminarisation theory presented by CEBECI and SMITH (1974). For relaminarisation they require the parameter K > 2 to 3 * 10^{-6}, where $K = \frac{v}{V^2}\frac{dV}{dx}$.

The dimensionless boundary layer thickness calculated by the method of Thwaites was found to be of the order of 10^{-3} for the first estimate which was assumed to demonstrate that further boundary layer correction was not required.

4 EXPERIMENTAL VERIFICATION

A physical model of the weir was constructed from steel finished with enamel paint to minimise protrusions into the flow.

Fourteen piezometric tappings were positioned along the side of the weir, in order to measure the pressure profile along the surface. A pitot static tube and point gauge were used to measure internal velocity and pressure distributions and the surface profile respectively.

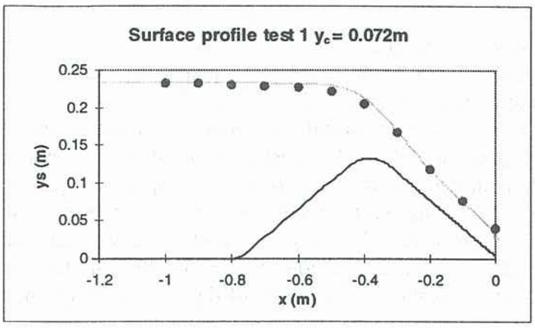

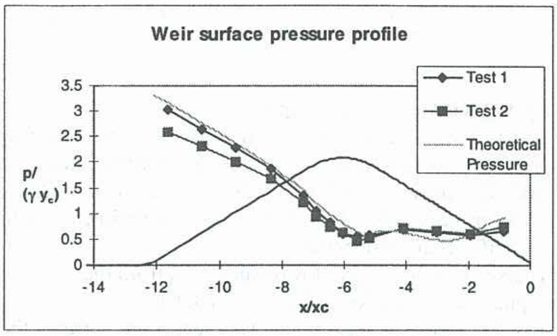

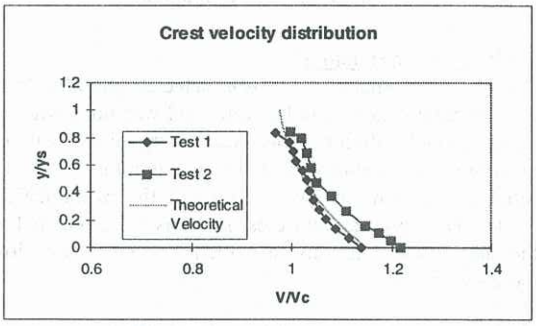

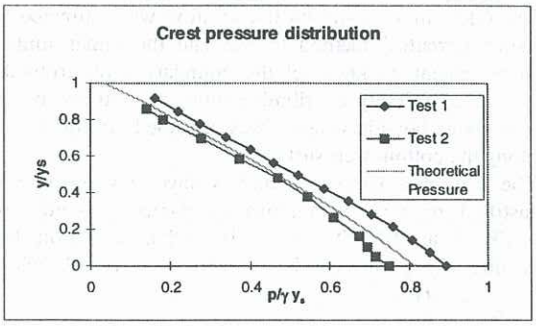

5 CONCLUSIONS

The numerical solution of the flow over a streamlined weir, allows the characteristics of the flow, surface profile, velocity and pressure distribution and flow momentum, to be calculated.

A numerical smoothing technique was found necessary to stabilise the correction of the water surface profile in the region of critical depth.

Two alternative conditions were applied to the downstream boundary, namely a hydrostatic pressure distribution, and a vortex of radius R. It was found that the hydrostatic model was in better agreement with experiment.

The use of Thwaites' method to estimate the boundary layer size, and the comparison of the model solution with experimental results indicates that the potential flow assumptions did not significantly alter the solution from real fluid flow.

In conclusion, it was found that the potential flow solution presented, based on an inverse method of solution of Laplace's equation converged mathematically and compared well with experimental data.

REFERENCES

Thom, A. and Appelt, C.J. *Field Computations in Engineering and Physics,* Van Nostrand, London 1961.

Domínguez, F.J. *Hidráulica,* Ed. Universitaria, Santiago, Chile, 1974.

Lafara, R.L. *Computer Methods for Science and Engineering,* Hayden book Co., 1973

Montes, J.S. *Irrotational Flow and Real Fluid Effects Under Planar Sluice Gates,* Journal of Hydraulic Engineering, ASCE, March 1997, Vol.123, No.3

Lauck, August *Überfall uber ein Wehr,* University of Berlin, Institute of Applied Mathematics, 1925

Thwaites, B. *Approximate Calculation of the Boundary Layer,* Aeronautical Quarterly, London 1949 pp.245-280

Cebeci, T and Smith, M.O., *Analysis of Turbulent Boundary Layer,* Academic Press, New York, 1974